



# Non-invasive Assessment of Subclinical Renal Parenchymal Changes in Chronic Hepatitis B Virus By T1 Mapping Magnetic Resonance Imaging

Serçin Özkök<sup>1</sup>, Ayşenur Buz<sup>1</sup>, Servet Erdemli<sup>1</sup>, Gülşah Şaşak Kuzgun<sup>2</sup>, Ahmet Aslan<sup>1</sup>

<sup>1</sup>Department of Radiology, Göztepe Training and Research Hospital, İstanbul Medeniyet University, İstanbul, Turkey

<sup>2</sup>Department of Nephrology, Göztepe Training and Research Hospital, İstanbul Medeniyet University, İstanbul, Turkey

**Background:** Renal parenchymal changes are seen in chronic hepatitis B virus (HBV) infection, and its disease diagnosis should be confirmed by renal biopsy, which is an invasive technique. Apparent-T1 mapping magnetic resonance imaging (MRI) is an established imaging technique that assesses subclinical tissue injury without using a contrast agent.

**Aims:** To investigate the early stage subclinical renal changes without apparent renal dysfunction in patients with chronic HBV infection by renal apparent-T1 mapping MRI.

**Study Design:** A cross-sectional study.

**Methods:** This study included 45 participants with normal kidney function, wherein 25 have biopsy-proven chronic HBV hepatitis and 20 are healthy individuals. Liver and kidney biochemical tests were performed within 1 month before the MRI scan, and the estimated glomerular filtration rate was calculated by diet modification in renal

disease formula. Breath-hold, electrocardiogram-gated Modified Look-Locker Imaging sequence was acquired in the coronal plane without contrast agent administration. Apparent-T1 mapping value was measured by manually drawing a region of interest in six points for both kidneys by two observers. Apparent-T1 mapping values were compared between the two groups.

**Results:** The mean apparent-T1 mapping values of the kidneys were significantly higher in patients with chronic HBV infection compared to the control group (1445 ± 129 ms vs. 1306 ± 115 ms,  $P = 0.003$ ). Inter-class correlation coefficient measurement analysis showed excellent agreement.

**Conclusion:** Renal apparent-T1 mapping MRI may help show the early stage of renal parenchymal disease without apparent renal dysfunction in chronic HBV infection.

## INTRODUCTION

Hepatitis B virus (HBV) infection is a worldwide health problem that affects >350 million HBV carriers that causes >600,000 deaths annually due to associated liver disease.<sup>1</sup> The liver disease in HBV infection is related to the immunologic response severity of the host toward the viral agent.<sup>2</sup> Additionally, renal parenchymal disease can be seen during the infection course.<sup>3</sup> Triggered apoptotic injury toward the renal tubular cells by cytokines, viruses, and antigens may be responsible for renal injury and parenchymal disease in chronic HBV infection.<sup>4-6</sup> Therefore, revealing whether the kidneys are primarily or secondary affected by HBV infection is important since it will determine the treatment and the kidney disease prognosis. Parenchymal kidney disease is often subclinical

and clinical biomarkers, such as estimated glomerular filtration rate (eGFR) and albuminuria, tend to be worsened in later disease period.

The exact diagnosis of the renal disease consists of antigen-antibody complex detection in biopsy samples via immunofluorescence microscopy.<sup>7</sup> Unfortunately, histopathological sampling may not be applicable because of the difficulties (small sample error and technique difficulties) and complications (bleeding, gross hematuria, perinephric hematoma, and arteriovenous fistulas).<sup>8</sup> These disadvantages of this gold-standard diagnostic test prevent its widespread use in daily practice and its acceptance as a screening test. Additionally, patients with normal kidney function tests cannot be a candidate for renal biopsy. Therefore, developing a non-invasive diagnostic test to assess the injury (acute vs. chronic),



Corresponding author: Serçin Özkök, Department of Radiology, Göztepe Training and Research Hospital, İstanbul Medeniyet University, İstanbul, Turkey  
e-mail: sercinbas2005@gmail.com

Received: June 24, 2021 Accepted: November 12, 2021 Available Online Date: March, 14, 2022 • DOI: 10.4274/balkanmedj.galenos.2021.2021-6-133

Available at [www.balkanmedicaljournal.org](http://www.balkanmedicaljournal.org)

ORCID iDs of the authors: S.Ö. 0000-0002-2176-5278; A.B. 0000-0003-1324-2810; S.E. 0000-0001-5545-768X; G.Ş.K. 0000-0003-4395-4368; A.A. 0000-0003-1433-6149.

Cite this article as:

Özkök S, Buz A, Erdemli S, Şaşak Kuzgun G, Aslan A. Non-invasive Assessment of Subclinical Renal Parenchymal Changes in Chronic Hepatitis B Virus By T1 Mapping Magnetic Resonance Imaging. *Balkan Med J.*; 2022; 39(2):115-20.

Copyright@Author(s) - Available online at <http://balkanmedicaljournal.org/>

fibrosis, and kidney inflammation without using a contrast agent or tissue sampling is essential. Recent applications of renal T1 mapping magnetic resonance imaging (MRI) for non-invasive tissue assessment without contrast media is a promising option for predicting acute and chronic parenchymal renal disease.<sup>9-15</sup>

This study aimed to investigate the subclinical renal parenchymal injuries without apparent renal dysfunction in patients with chronic HBV infection using renal apparent-T1 mapping MRI.

## MATERIALS AND METHODS

This cross-sectional study was approved by the Institutional Review Board and written informed consent was obtained.

### Patient Selection

This study included 25 patients with histopathologically proven non-cirrhotic chronic HBV hepatitis and 20 healthy subjects without apparent kidney disease. Liver and kidney function tests (serum blood urea nitrogen [BUN], creatinine, sodium [Na], potassium [K], albumin, white blood cell [WBC], hemoglobin [Hgb], alanine transaminase [ALT], aspartate transaminase [AST], gamma-glutamyl transferase [GGT], and C-reactive protein [CRP] levels) and serum hepatitis B surface antigen (Hbs Ag) levels were revealed from the hospital information system. For each participant, eGFR was calculated by the Modification of Diet in Renal Disease formula. Abdominal ultrasound was performed within 1 month before the MRI scan. Participants with a history of cardiovascular disease, diabetes mellitus, hypertension, hyperlipidemia, autoimmune diseases (i.e., Buerger's disease, Behcet's syndrome, Takayasu's arteritis, systemic lupus, autoimmune arthritis, and scleroderma), chronic or acute renal dysfunction (including proteinuria, elevated kidney function test parameters, and chronic parenchymal changes) were excluded from the study. Patients who had liver tissue sampling revealed within 1 year before the MRI scan were included in the study. Patients who were diagnosed within the last year were excluded. Participants who had antiviral

medication in the previous 6 months and decreased hemoglobin levels were also excluded from the study since decreased hemoglobin levels may cause apparent-T1 value elongation and HBV antiviral treatment may also cause renal dysfunction.<sup>16,17</sup> MRI studies with severe artifacts were also excluded.

### Magnetic Resonance Imaging

All MRIs were performed with a 1.5 Tesla magnet field scanner (Signa 450W; GE Medical Systems, Milwaukee, WI, USA) using a 32-channel phased-array surface coil. Breath-hold, electrocardiogram-gated Modified Look-Locker Imaging (MOLLI) sequence was acquired in the coronal axis of both kidneys. The MOLLI sequence is inversion-based, which takes 3 slices at 7 different saturation times and 11 heartbeat durations. Typical parameters of MOLLI sequence are as follows: TR/TE of 2.8/1.2 ms, slice thickness/spacing of 8.0/5.0 mm, first inversion time (TI) of 200 ms, TI increment of 80 ms, a field of view of 380 × 300 mm, acquisition matrix of 160 × 128, flip angle of 65°, and bandwidth of 125 kHz. Coronal T2 weighted images were also revealed to differentiate the cortex and the medulla. Typical parameters are as follows: TR/TE of 3/1 ms, slice thickness/spacing of 6/2 mm, a field of view of 350 mm, acquisition matrix of 224 × 224, flip angle of 60°, and bandwidth of 111 kHz. The total scanning time was between 10 to 15 min and no contrast agent was injected during the scanning.

Images taken with MOLLI sequences were automatically processed in the MRI device and T1 maps were produced with automatic software loaded on the device side. The renal apparent-T1 mapping value was automatically measured for each kidney on a workstation (Advantage Workstation, GE Healthcare, Milwaukee, WI, USA) and is recorded. The region of interest (ROI) was manually placed in six different regions (upper, middle, and lower poles for each kidney in the renal cortex and medulla) by two observers who were blinded to patients' data on coronal images (Figure 1). Perirenal abdominal fat tissue and renal sinus

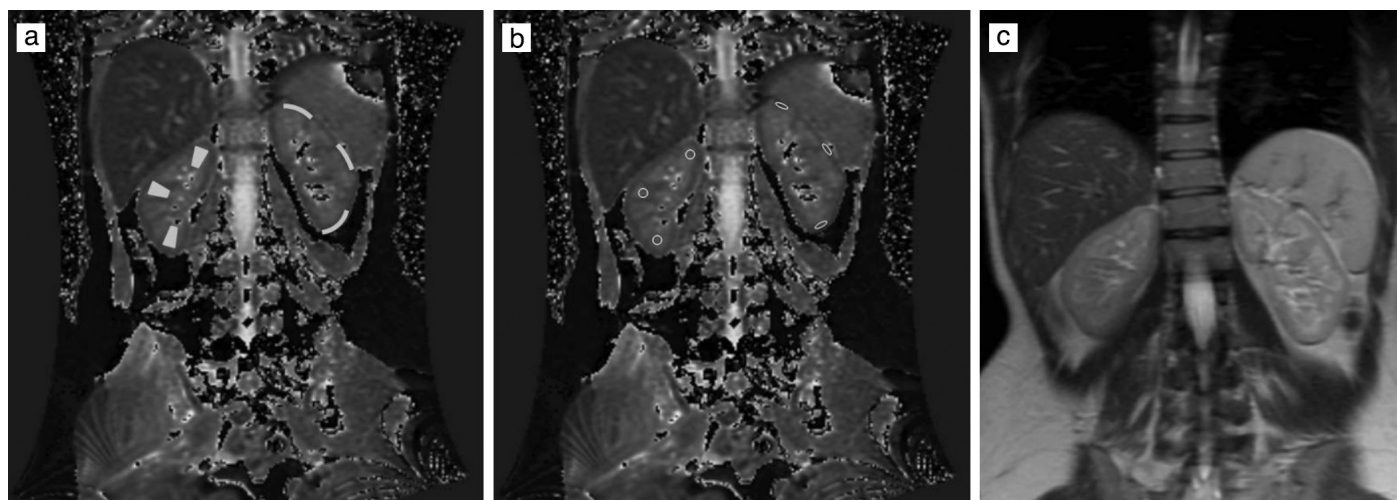


FIG 1. Coronal T1 mapping image demonstrates renal medulla (right kidney) and renal cortex (left kidney) in upper, middle, and lower poles (a). The ROI is located in the renal medulla (right kidney) and renal cortex (left kidney) in the upper, middle, and lower poles (b). T2-weighted image in coronal plane shows the renal cortex and medulla of both kidneys (c).

fat were not included in ROI measurements to avoid partial volume averaging artifacts.

### Statistics

Obtained data were analyzed using the Statistical Package for the Social Sciences version 20.0 software (IBM Corporation, Armonk, NY, USA). The mean values of two observers' measurements were used to compare apparent-T1 values. Results were expressed as the mean  $\pm$  standard deviation and considered significant if  $P < 0.05$ . The mean and standard deviation values were used for the presentation of descriptive values. The Shapiro–Wilk normality test was applied to evaluate the normality of the obtained data. The Student's T-test was used to compare the apparent-T1 mapping values and other variables between groups and the dependent T-test within groups. The analysis of variance was performed to assess the correlation between different ROIs of the renal cortex and medulla. Pearson's correlation coefficient was performed to evaluate the correlation between apparent-T1 mapping values and serum biochemistry parameters. Reproducibility and agreement were evaluated with inter-class correlation (ICC) coefficients. ICC coefficient of  $>0.8$  indicates excellent agreement,  $0.8-0.6$  indicates substantial agreement,  $0.6-0.4$  indicates moderate agreement, and  $<0.4$  indicates poor agreement.<sup>18</sup>

### RESULTS

The mean age of 25 patients with non-cirrhotic chronic HBV hepatitis (12 females and 13 males) was  $47.64 \pm 16.41$  (20–65) years, whereas  $35.84 \pm 11.96$  (23–69) years in 20 healthy individuals (9 females and 11 males) ( $P = 0.281$ ). No statistically significant difference was found between the chronic HBV hepatitis and control groups in terms of mean GFR, serum creatinine, serum BUN, Na, K, albumin, WBC, and Hgb levels

( $p$ -values were 0.551; 0.971; 0.888; 0.733; 0.608; 0.788; 0.957, and 0.805, respectively). A significant difference was found between the two groups in the mean serum ALT, AST, GGT, and CRP levels ( $p$ -values were 0.001, 0.047, 0.044, and 0.0001, respectively). The mean Hbs Ag level was  $4984 \pm 1017$  (IU/mL) in the patient group. The demographic data and laboratory findings are shown in Table 1.

The mean apparent T1 values of the renal cortex, medulla, and entire kidney were  $1578.56 \pm 112.63$  ms,  $1253.79 \pm 116.45$  ms, and  $1416.17 \pm 100.73$  ms, respectively, in the patient group, whereas that of the control group were  $1455.93 \pm 102.59$  ms,  $1133.56 \pm 80.06$ ms, and  $1294.75 \pm 82.33$ ms, respectively. The mean value of the cortex was significantly higher than the medulla in the patient and control groups ( $P = 0.0001$  and  $P = 0.0001$ , respectively). The mean apparent-T1 mapping values of the renal cortex, medulla, and entire kidney were significantly higher in the patient group compared to the control group ( $P = 0.0004$ ;  $P = 0.0002$ ;  $P = 0.0001$ , respectively) (Table 2, Figure 2). No significant differences were found between the differences of T1 mapping values using three different ROIs in patients with chronic HBV hepatitis (Table 3). Measurements of the renal cortex and medulla of both groups are shown in Table S1 and S2. No significant correlation was found between serum liver and kidney function parameters, GFR, and T1 mapping value in the patient group (Table 4). The ICC analysis of two observers revealed an excellent agreement in the measurements of apparent-T1 mapping of the kidneys ( $1431 \pm 138$  ms vs.  $1406 \pm 81$  ms, ICC = 0.831, 95 % confidence interval = 0.583–0.931,  $P = 0.001$ ).

### DISCUSSION

Technological improvements of MRI sequences monitored the physiological changes and renal parenchymal diseases, such

TABLE 1. Demographic Information and Biochemical Parameters of Patient and Control Groups.

Characteristic	Chronic HBV Group (n = 25)	Control Group (n = 20)	P-value
Age (year)	$47.64 \pm 16.41$ (20–65)	$35.84 \pm 11.96$ (23–69)	0.281
Serum Creatinine ( $\mu\text{mol/L}$ )	$0.79 \pm 0.11$	$0.79 \pm 0.1$	0.971
BUN (mg/dL)	$20.12 \pm 6.15$	$19.84 \pm 6.78$	0.888
Na (mmol/L)	$139.56 \pm 1.89$	$139.37 \pm 1.73$	0.733
K (mEq/L)	$4.34 \pm 0.21$	$4.37 \pm 0.21$	0.608
ALT (U/L)	$61.2 \pm 37.66$	$19.32 \pm 8.59$	0.0001*
AST (U/L)	$34.36 \pm 28.56$	$20.74 \pm 1.34$	0.047*
GGT (U/L)	$31.12 \pm 23.5$	$19.52 \pm 7.05$	0.044*
CRP (mg/L)	$0.42 \pm 0.2$	$0.23 \pm 0.07$	0.0001*
Albumin (g/dL)	$3.95 \pm 0.72$	$3.89 \pm 0.81$	0.788
WBC ( $\times 10^9/\text{L}$ )	$6.73 \pm 0.14$	$6.69 \pm 1.71$	0.957
HbG (g/dL)	$13.57 \pm 1.69$	$13.68 \pm 1.89$	0.805
eGFR (mL/min/1.73 m <sup>2</sup> )	$111.86 \pm 18.43$	$114.83 \pm 10.79$	0.551

Results are presented as mean  $\pm$  SD. P: P-value of independent samples Student's t-tests. P\* value is significant if  $<0.05$ .

BUN: blood urea nitrogen; ALT: alanine transaminase; AST: aspartate transaminase; GGT: Gamma-glutamyl transferase; CRP: C-reactive protein; WBC: white blood cell; HbG: hemoglobin, Na: sodium, K: potassium, eGFR: estimated glomerular filtration rate.

**TABLE 2.** T1 Mapping Values of Renal Cortex, Medulla, and Entire Kidney for Patient and Control Groups.

	Chronic HBV Group (n = 25)	Control Group (n = 20)	P-value
<b>Renal Cortex</b>	1578.56 ± 112.63	1455.93 ± 102.59	0.0004*
<b>Renal Medulla</b>	1253.79 ± 116.45	1133.56 ± 80.06	0.0002*
<b>Entire Kidney</b>	1416.17 ± 100.73	1294.75 ± 82.33	0.0001*
<b>P-value</b>	0.0001	0.0001	

Results are presented as mean ± SD. P: P-value of independent samples Student's t-tests. P\* value is significant if <0.05.

**TABLE 3.** Mean T1 Mapping Values of Three Different ROIs In Patients with Chronic HBV Hepatitis.

	T1 Value-ROI 1 Upper pole	T1 Value-ROI 2 Mid-pole	T1 Value-ROI 3 Lower pole	P-value
<b>Renal Cortex</b>	1609.16 ± 157.55	1565.01 ± 131.45	1558.51 ± 154.72	0.443
<b>Renal Medulla</b>	1313.39 ± 205.45	1229.77 ± 95.64	1218.19 ± 167.87	0.086

Results are presented as mean ± SD. P: P-value of independent samples ANOVA test. P-value is significant if <0.05.

**TABLE 4.** Correlation of the Study Parameters with the Mean T1 Mapping Value in Patients with Chronic HBV Hepatitis.

Characteristic	r	P-value
<b>Serum Creatinine (µmol/L)</b>	0.3	0.145
<b>BUN (mg/dL)</b>	0.202	0.333
<b>Na (mmol/L)</b>	-0.007	0.972
<b>K (mEq/L)</b>	0.271	0.191
<b>ALT (U/L)</b>	0.147	0.483
<b>AST (U/L)</b>	-0.06	0.775
<b>GGT (U/L)</b>	-0.198	0.343
<b>CRP (mg/L)</b>	0.026	0.902
<b>Albumin (g/dL)</b>	-0.295	0.153
<b>WBC (x10<sup>9</sup>/L)</b>	0.340	0.960
<b>HbG (g/dL)</b>	-0.034	0.871
<b>eGFR (mL/min/1.73m<sup>2</sup>)</b>	-0.031	0.894

Results are presented as mean ± SD. P: p-value of Pearson's correlation test  
Abbreviations: BUN: blood urea nitrogen; ALT: alanine transaminase; AST: aspartate transaminase; GGT: Gamma-glutamyl transferase; CRP: C-reactive protein; WBC: white blood cell; HbG: hemoglobin; Na: sodium; K: potassium; eGFR: estimated glomerular filtration rate

**Apparent-T1 Value (ms)**

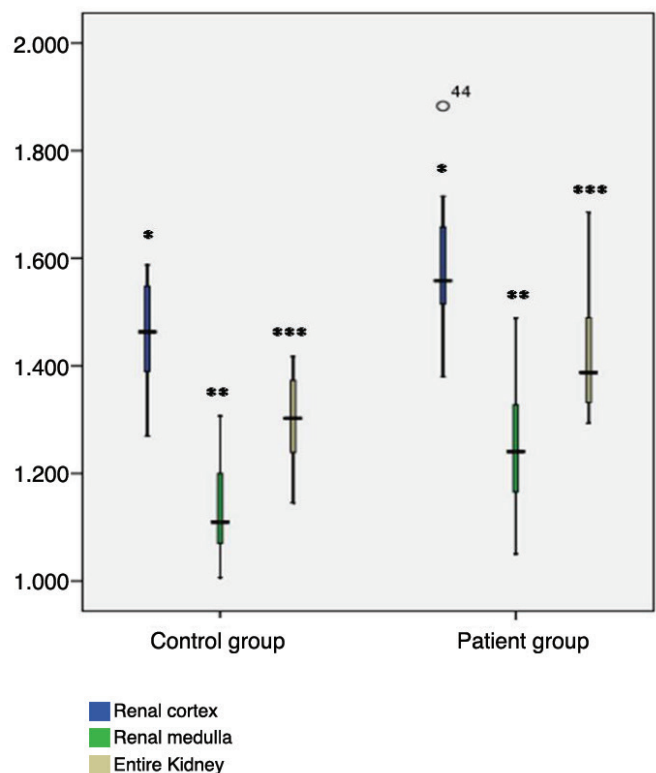


**FIG. 2.** Comparison between the mean apparent-T1 mapping values of the renal cortex, medulla, and entire kidney. For the box and whiskers plots, the upper and lower borders of the box represent the upper and lower quartiles. The middle horizontal line represents the median. The upper and lower whiskers represent the maximum and minimum values of non-outliers. Extra dots represent outliers.

as fibrosis and edema.<sup>19-25</sup> The usefulness of the T1 mapping technique in renal imaging and the specific T1 mapping values for primary and secondary renal diseases have been published in recent years.<sup>9,11,13,15,26-29</sup> Renal cortical and medullary T1 mapping values can be used as a diagnostic, monitoring, and pharmacodynamic/response biomarker to assess the course of renal parenchymal diseases without using a contrast agent.<sup>30</sup> However, to our knowledge, no study has been presented in the English medical literature that investigated the renal T1 mapping values of patients with non-cirrhotic chronic HBV infection that may imply early stage renal injury. As a widely accepted imaging technique in cardiac imaging, apparent-T1 mapping MRI without contrast agent is commonly used to assess edema, infarction, amyloid infiltration, and fibrosis.<sup>31</sup> However, clinical application of T1 mapping in renal imaging is limited and no study has assessed the renal parenchymal changes in chronic liver disease.

The literature suggested that the T1 mapping MRI is an appropriate and non-invasive imaging tool for assessing either acute<sup>27,28</sup> or chronic changes of kidney parenchyma and progression of fibrosis<sup>9,29</sup> that is confirmed by tissue sampling in animal models.

Chronic renal changes were demonstrated by the T1 mapping technique and are well correlated to fibrosis progression in unilateral ureteral obstruction.<sup>9,29</sup> T1 mapping MRI may be an appropriate non-invasive imaging modality for assessing acute kidney injury allograft kidney.<sup>22,24</sup> Rankin et al.<sup>12</sup> revealed that cortical T1 mapping values of the kidneys were higher in renal transplant recipients compared to healthy volunteers in patients with heart failure. Friedli et al.<sup>9</sup> demonstrated that the T1 mapping values of renal parenchyma were correlated to interstitial fibrosis and inflammation in animal models and kidney allograft recipients compared to healthy kidneys; however, no correlation was found between T1 mapping values and inflammation. Additionally, Peperhove et al.<sup>15</sup> studied renal T1 mapping imaging in patients with solid organ transplantation 3 and 6 months after transplantation, which compared 49 renal transplant recipients and 52 lung transplantation to healthy individuals. Increased T1 mapping values of the renal cortex at 3 and 6 months after transplantation correlated with eGFR. T1 mapping values of the kidneys were more prominent in patients with kidneys than lung transplantation. Huang et al.<sup>32</sup> showed increased T1 mapping values of the cortex and medulla in kidneys transplantation compared to healthy volunteers, and T1 mapping values of the renal cortex in both groups showed a strong correlation with eGFR. A recent study by Beck-Tolly et al.<sup>33</sup> also demonstrated a significant association between the severity of interstitial fibrosis and increased apparent-T1 mapping value in renal cortex allograft kidney. Increased cortical apparent-T1 mapping values were also found to be reflected by impaired graft function and proteinuria.<sup>33</sup>

Cortical apparent-T1 mapping value is significantly increased in patients with Immunoglobulin A nephropathy compared to healthy participants in a recent study.<sup>26</sup> Not only in acute kidney injury but also chronic kidney disease, T1 mapping values were increased and showed a positive correlation with eGFR.<sup>20,21</sup> Gillis et al. revealed a higher cortical T1 mapping value and whole kidney in chronic kidney disease. A positive correlation was found between the T1 mapping value and eGFR.<sup>13</sup> Fox et al. also found similar results in patients with chronic kidney disease.<sup>15</sup> T1 mapping value of the renal cortex and medulla was higher at both 1.5 and 3 Tesla magnet fields MRI. Our study revealed a significantly increased renal apparent-T1 mapping value in patients with chronic HBV infection without apparent renal dysfunction compared to the control group. Participants in both groups had no apparent renal dysfunction as evaluated by eGFR, serum creatinine, serum BUN, Na, K, albumin, and WBC levels. Additionally, the participants had no proteinuria, hematuria, and elevated systemic blood pressure, which denotes renal parenchymal disease. Our study results support that prolonged T1 relaxation time could be used as a non-invasive imaging technique to detect subclinical renal parenchymal changes in chronic liver disease without a contrast agent, which is concordant with the literature.<sup>12-15,26-29,33</sup> We can emphasize that renal T1 mapping values can be used as a predictor of kidney function in an earlier stage than proteinuria or eGFR prolongation seen in later stages. The ICC analysis of the measurements of renal apparent-T1 mapping showed excellent

agreement. Similar results were also reported in the study by Dekkers et al.<sup>25</sup>

However, our study has some limitations. The most important limitation is that the repeatability assessment of the measurement in healthy volunteers on two different days was not performed. Additionally, we did not assess whether the apparent T1 measurement is valid and accurate using a valid T1 phantom. Moreover, we have a small sample size. The study cohort is limited; however, we showed a high inter-observer agreement of measurements of the renal T1 mapping with a sufficient number of samples. Insufficient histopathological findings are another limitation. However, patients with normal kidney function tests cannot be a candidate for renal biopsy in clinical practice. Further studies that correlated with histopathological findings should be planned.

In conclusion, apparent-T1 mapping MRI could be a useful and reliable tool in the early diagnosis and monitoring of parenchymal renal diseases.

**Ethics Committee Approval:** All procedures performed in studies involving human participants were in accordance with the ethical standards of the institutional and/or national research committee and with the 1964 Helsinki declaration and its later amendments or comparable ethical standards. This article does not contain any studies with human participants or animals performed by any of the authors.

**Data Sharing Statement:** The data that support the findings of this study are available from the corresponding author upon reasonable request.

**Author Contributions:** Concept- S.O. ; Design- S.O, A.A.; Supervision –A.A.; Data Collection and Processing –S.O., A.B.,S.E.; Analysis and/or Interpretation – S.O., G.S.K.; Writing –S.O.

**Conflict of Interest:** No conflict of interest was declared by the authors.

**Funding:** The authors declared that tis study received no financial support.

**Acknowledgments:** We thank GE Healthcare, Turkey, for providing the T1 mapping, MOLLI sequence for our research.

**Supplementary:** <https://balkanmedicaljournal.org/uploads/pdf/balkanmedj.galenos.2021.2021-6-133-Supplementary.pdf>

## REFERENCES

- Goldstein ST, Zhou F, Hadler SC, Bell BP, Mast EE, Margolis HS. A mathematical model to estimate global hepatitis B disease burden and vaccination impact. *Int J Epidemiol.* 2005; 34:1329-1339. [\[Crossref\]](#)
- Meuleman P, Libbrecht L, Wieland S, et al. Immune suppression uncovers endogenous cytopathic effects of the hepatitis B virus. *J Virol.* 2006;80:2797-807. [\[Crossref\]](#)
- Apurva S, Deepak A. Spectrum of hepatitis B and renal involvement. *Liver Int.* 2018;38:23-32. [\[Crossref\]](#)
- Bhimma R, Coovadia HM. Hepatitis B virus-associated nephropathy. *Am J Nephrol.* 2004;24:198-211. [\[Crossref\]](#)
- Lai KN, Ho RT, Tam JS, Lai FM. Detection of hepatitis B virus DNA and RNA in kidneys of HBV related glomerulonephritis. *Kidney Int.* 1996;50:1965-1977. [\[Crossref\]](#)
- Deng CL, Song XW, Liang HJ, Feng C, Sheng YJ, Wang MY. Chronic hepatitis B serum promotes apoptotic damage in human renal tubular cells. *World J Gastroenterol.* 2006;12:1752-6. [\[Crossref\]](#)
- Lai KN, Li PK, Lui SF, et al. Membranous nephropathy related to hepatitis B virus in adults. *N Engl J Med.* 1991;324:1457-1463. [\[Crossref\]](#)
- Jiang K, Ferguson CM, Lerman LO. Noninvasive assessment of renal fibrosis by magnetic resonance imaging and ultrasound techniques. *Transl Res.* 2019;209:105-120. [\[Crossref\]](#)

9. Friedli I, Crowe LA, Berchtold L, et al. New magnetic resonance imaging index for renal fibrosis assessment: a comparison between diffusion-weighted imaging and T1 mapping with histological validation. *Sci Rep*. 2016;6:30088. [\[Crossref\]](#)
10. Beck-Töly A, Eder M, Beitzke D, et al. Magnetic Resonance Imaging for Evaluation of Interstitial Fibrosis in Kidney Allografts. *Transplant Direct*. 2020;6:e577. [\[Crossref\]](#)
11. Cox EF, Buchanan CE, Bradley CR, et al. Multiparametric Renal Magnetic Resonance Imaging: Validation, Interventions, and Alterations in Chronic Kidney Disease. *Front Physiol*. 2017;8:696. [\[Crossref\]](#)
12. Rankin AJ, Allwood-Spiers S, Lee MMY, et al. Comparing the interobserver reproducibility of different regions of interest on multi-parametric renal magnetic resonance imaging in healthy volunteers, patients with heart failure and renal transplant recipients. *MAGMA*. 2020;33:103-112. [\[Crossref\]](#)
13. Gillis KA, McComb C, Patel RK, et al. Non-Contrast Renal Magnetic Resonance Imaging to Assess Perfusion and Corticomedullary Differentiation in Health and Chronic Kidney Disease. *Nephron*. 2016;133:183-192. [\[Crossref\]](#)
14. Wolf M, de Boer A, Sharma K, et al. Magnetic resonance imaging T1- and T2-mapping to assess renal structure and function: a systematic review and statement paper. *Nephrol Dial Transplant*. 2018;33:ii41-ii50. [\[Crossref\]](#)
15. Peperhove M, VoChieu VD, Jang MS, et al. Assessment of acute kidney injury with T1 mapping MRI following solid organ transplantation. *Eur Radiol*. 2018;28:44-50. [\[Crossref\]](#)
16. Rosmini S, Bulluck H, Abdel-Gadir A, et al. The Effect of Blood Composition on T1 Mapping. *JACC Cardiovasc Imaging*. 2019;12:1888-1890. [\[Crossref\]](#)
17. Jang E, Lee JK, Inn KS, Chung EK, Lee KT, Lee JH. Renal Dysfunction and Tubulopathy Induced by High-Dose Tenofovir Disoproxil Fumarate in C57BL/6 Mice. *Healthcare (Basel)*. 2020;8:417. [\[Crossref\]](#)
18. Landis JR, Koch GG. The measurement of observer agreement for categorical data. *Biometrics*. 1977;33:159-174. [\[Crossref\]](#)
19. Lanzman RS, Wittsack HJ, Martirosian P, et al. Quantification of renal allograft perfusion using arterial spin labeling MRI: initial results. *Eur Radiol*. 2010;20:1485-1491. [\[Crossref\]](#)
20. Prasad PV. Functional MRI of the kidney: tools for translational studies of pathophysiology of renal disease. *Am J Physiol Ren Physiol*. 2015;290:F958-974. [\[Crossref\]](#)
21. Pohlmann A, Hentschel J, Fechner M. High temporal resolution parametric MRI monitoring of the initial ischemia/reperfusion phase in experimental acute kidney injury. *PLoS One*. 2013;8:e57411. [\[Crossref\]](#)
22. Lanzman RS, Ljimani A, Pentang G, et al. Kidney transplant: functional assessment with diffusion-tensor MR imaging at 3T. *Radiology*. 2013;266:218-225. [\[Crossref\]](#)
23. Thoeny HC, De Keyzer F. Diffusion-weighted MR imaging of native and transplanted kidneys. *Radiology*. 2011;259:25-38. [\[Crossref\]](#)
24. Hueper K, Gutberlet M, Rodt T, et al. Diffusion tensor imaging and tractography for assessment of renal allograft dysfunction-initial results. *Eur Radiol*. 2011;21:2427-2433. [\[Crossref\]](#)
25. Dekkers IA, de Boer A, Sharma K, et al. Consensus-based technical recommendations for clinical translation of renal T1 and T2 mapping MRI. *MAGMA*. 2020;33:163-176. [\[Crossref\]](#)
26. Graham-Brown MP, Singh A, Wormleighton J, et al. Association between native T1 mapping of the kidney and renal fibrosis in patients with IgA nephropathy. *BMC Nephrology*. 2019;20:256. [\[Crossref\]](#)
27. Hueper K, Peperhove M, Rong S, et al. T1-mapping for assessment of ischemia-induced acute kidney injury and prediction of chronic kidney disease in mice. *Eur Radiol*. 2014;24:2252-2260. [\[Crossref\]](#)
28. Sheung-Fat K, Hon-Kan Yip, Yen-Yi Zhen, et al. Severe bilateral ischemic reperfusion renal injury: hyperacute and acute changes in apparent diffusion coefficient, T1, and T2 mapping with immunohistochemical correlations. *Sci Rep*. 2017;7:1725. [\[Crossref\]](#)
29. Genwen Hu, Liang W, Wu M, et al. Comparison of T1 Mapping and T1rho Values with Conventional Diffusion Weighted Imaging to Assess Fibrosis in a Rat Model of Unilateral Ureteral Obstruction. *Acad Radiol*. 2019;26:22-29. [\[Crossref\]](#)
30. FDA-NIH Biomarker Working Group. BEST (Biomarkers, EndpointS, and other Tools) Resource [Internet]. Silver Spring (MD): Food and Drug Administration (US); 2016-. Available from: <https://www.ncbi.nlm.nih.gov/books/NBK326791/> Co-published by National Institutes of Health (US), Bethesda (MD). [\[Crossref\]](#)
31. Radenkovic D, Weingärtner S, Ricketts L, et al. T1 mapping in cardiac MRI. *Heart Fail Rev*. 2017;22:415-430. [\[Crossref\]](#)
32. Huang Y, Sadowski EA, Artz NS, et al. Measurement and comparison of T1 relaxation times in native and transplanted kidney cortex and medulla. *J Magn Reson Imaging*. 2011;33:1241-1247. [\[Crossref\]](#)
33. Beck-Töly A, Eder M, Beitzke D, et al. Magnetic Resonance Imaging for Evaluation of Interstitial Fibrosis in Kidney Allografts. *Transplant Direct*. 2020;15:e57vv7. [\[Crossref\]](#)